

# Spline-constrained tool-path planning in five-axis flank machining of ruled surfaces

Chih-Hsing Chu<sup>1</sup> · Hsin-Ta Hsieh<sup>1</sup> · Chen-Han Lee<sup>2</sup> · Changya Yan<sup>2</sup>

Received: 6 August 2014 / Accepted: 21 April 2015 / Published online: 1 May 2015  
© Springer-Verlag London 2015

**Abstract** Previous optimization-driven tool-path planning methods provide an effective approach to machining error control in five-axis flank milling of ruled surfaces. However, the finished part typically exhibits poor surface roughness. This paper proposes a new planning method for overcoming this problem. The proposed method generates a spline-curve-constrained tool path that produces minimized geometrical deviations on the machined surface, maintains satisfactory surface quality, and reduces the dimensionality in the solution space. A particle swarm optimization scheme was developed to determine the coefficients of the curve equations defining the constrained tool motion. A machining experiment was conducted and the measurement results validated the proposed method.

**Keywords** Five-axis machining · Flank milling · Spline interpolation · Tool-path planning · Particle swarm optimization

## 1 Introduction

Five-axis machining is an advanced manufacturing technology commonly used for creating complex geometries in the automobile, aerospace, mold-making, and energy industries. It offers higher shaping capability and productivity than

traditional three-axis machining does, with two rotational degrees of freedom in tool motion. Five-axis machining operations are classified into end milling and flank milling according to how the cutter removes stock material. In flank milling, the cutting edges along the cutter peripheral, generally of a cylindrical or conical shape, perform the cutting action. Tool-path planning in this operation remains challenging [1]. Completely eliminating tool overcut and undercut is highly difficult, if not impossible, when machining complex shapes. In practice, the finished surface is considered acceptable when the amount of geometrical deviations is within a given tolerance.

For reducing the geometrical deviations (not considering the errors induced physically such as cutter deflection and tool wear) produced in five-axis flank milling, numerous studies [2–8] have proposed various tool-path planning methods that can be classified into either a local or global approach [2]. The local approach [3–5] entails analyzing tool engagement conditions locally at the cutter location and developing geometric algorithms to separately adjust individual cutter locations for reducing the degree of deviations. Based on both simulation and experimental results, Chu et al. [9] showed that the local approach might not produce minimal deviations that accumulate on the entire finished surface. This effect becomes more significant as the distance between consecutive cutter locations increases. A global approach is thus necessary to adjust individual cutter locations simultaneously, because the tool motion linearly interpolated from consecutive cutter locations might yield a greater degree of geometrical deviations than that induced by a cutter location.

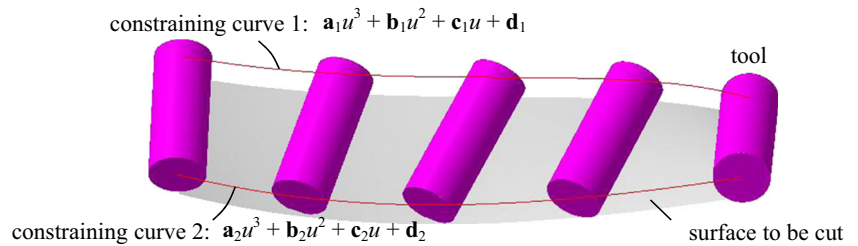
Hence, various optimization schemes [6–8] have been proposed for adjusting cutter locations simultaneously by applying an objective function to minimize the accumulated geometrical deviations of the finished surface. Experimental results have verified that the corresponding tool path produces

✉ Chih-Hsing Chu  
chchu@ie.nthu.edu.tw

<sup>1</sup> Department of Industrial Engineering and Engineering Management, National Tsing-Hua University, Hsinchu, Taiwan

<sup>2</sup> National NC Engineering Research Center, Huazhong University of Science and Technology, Wuhan, China

**Fig. 1** A tool path is constrained by two spline curves



smaller machining deviations. However, these methods demonstrate the following drawback: Both the tool center point and axis must be modified during the optimization process. Such modifications are particularly observable at the cutter locations around the surface regions of excessive twist, in which the surface is of low local developability [10]. Uneven modifications of the tool motion often result in poor surface quality on the finished part. Considering both geometrical precision and machining quality is necessary in tool-path planning.

This paper proposes a new tool-path planning method to serve this purpose. The proposed method involves imposing an intrinsic constraint on the tool motion during its optimization-driven modification process. Specifically, the tool path is described in the form of spline curves during the optimization process. Instead of adjusting individual cutter locations, a particle swarm optimization (PSO) algorithm is used to determine the coefficients of the curve equations by minimizing accumulated geometrical errors on the machined surface during the optimization process. Preserving the continuity of the tool motion facilitates maintaining high surface

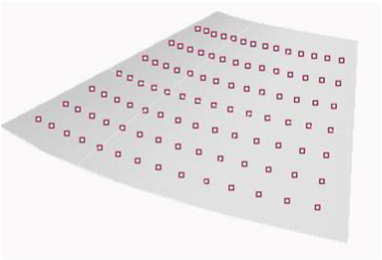
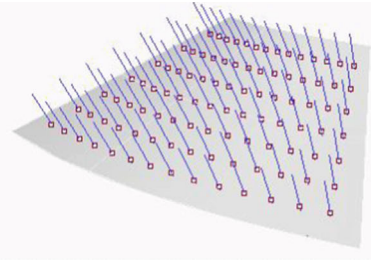
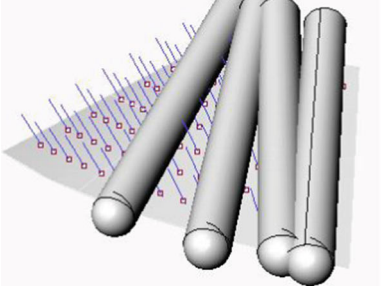
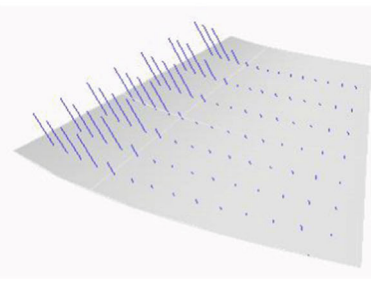
quality on the finished part. A five-axis machining test was conducted in this study by applying different tool paths to compare their effectiveness. Measurement data from a surface scanner revealed that, compared with previous methods, the proposed method generates a tool path that yields superior results in both geometrical errors and surface roughness.

## 2 Tool-path planning method

### 2.1 Tool-path planning driven by global optimization

A computer numerical control (CNC) tool path consists of a set of consecutive cutter locations. In current practice, the cutter generally follows a linearly interpolated tool motion between consecutive cutter locations. CNC spline interpolation technologies have been successfully developed for years, but their industrial use remains limited. In the five-axis flank milling of a ruled surface, the simplest method for tool-path planning is to allow the cutter to move along the surface rulings. The resultant path yields machining deviations when the surface is

**Fig. 2** Estimating machining deviations by the stock height method [2]

1. Generate sample points	2. Produce line segments at each sample point
	
3. Intersect the lines with the cutter	4. Calculate the accumulated deviations
	

**Table 1** Machining parameters in the tool path planning

Number of cutter locations	40
Cutter edge length	30 mm
Cutter radius	2 mm
Number of interpolations between cutter locations	10

twisted around a surface ruling or, more specifically, the surface is non-developable around the ruling [10]. Previous studies [3, 4] have applied geometric algorithms to adjust individual cutter locations in these surface regions. The adjustment can also change the tool motion between cutter locations. The number of accumulated deviations might not be minimal even if the cutter produces no errors at each cutter location. Thus, all cutter locations of a tool path must be adjusted simultaneously. This adjustment method is the global approach [9].

A cutter location is defined according to the cutter center point  $\mathbf{c}_i$  and cutter axis  $\mathbf{n}_i$ . Each vector ( $\mathbf{c}_i$  and  $\mathbf{n}_i$ ) contains three variables in 3D space. Thus, specifying a cutter location requires six variables. Assume that a tool path consists of  $N$  cutter locations. The solution space becomes  $6N$ -dimensional in the global approach, with  $N$  often used as a two-digit number in the machining of a curved surface. Searching for optima in such a highly non-linear domain is extremely difficult, if not impossible. The computational time is lengthy and the solution quality is occasionally poor; therefore, reducing the number of optimization variables is advantageous.

**2.2 Spline-constrained tool motion**

A feasible method for reducing the dimensionality in the solution space is to impose a motion pattern and the corresponding constraints while adjusting the cutter locations. More importantly, a continuous motion pattern produces a smooth tool path without creating excessive changes to the cutter locations during the optimization process. The part cut by the constrained tool path should exhibit higher surface quality than that cut by one that is unconstrained. This paper proposes an optimization scheme for realizing this concept in tool-path planning. As shown in Fig. 1, a tool path is defined according to two curves along which the two tool center points move. Assume both curves are represented using a cubic polynomial curve as

$$\mathbf{C}_i = \mathbf{a}_i u^3 + \mathbf{b}_i u^2 + \mathbf{c}_i u + \mathbf{d}_i, \text{ where } i = 1 \text{ and } 2 \quad (1)$$

**Table 2** Parameter settings in the PSO algorithm

Inertia weight	0.5
First learning factor	0.5
Second learning factor	0.5
Number of particles	100
Number of iterations	100

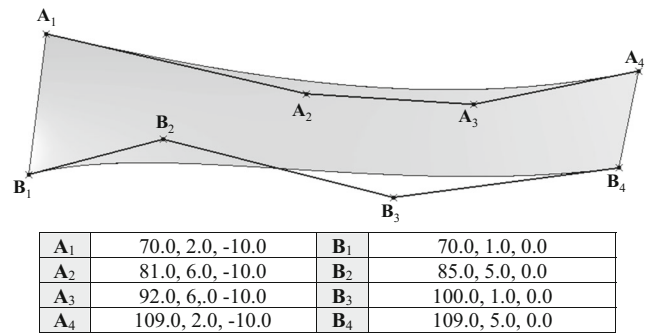


**Fig. 3** A test ruled surface and its control points

Each vector coefficient contains three variables. Completely describing a tool path of this form requires 24 variables. This number is much smaller than that of the tool path defined according to a set of discrete cutter locations.

**2.3 PSO algorithm**

As in most previous studies, the objective function was applied in the optimization scheme to be the accumulated geometrical deviations on the finished surface. Exact estimation of the machined geometry is highly complicated and might not be required. A previous study [2] proposed the stock height method for estimating the deviations approximately. The involved estimation process consists of four steps, as shown in Fig. 2. The design surface is first discretized into sample points. At each sampling point, two straight lines are extended along the positive and negative normal directions at the distance of the cutter radius. The lengths of these lines are updated after the cutter sweeps across them along a given tool path. The tool-swept surface is approximated by interpolating a finite number of tool positions between consecutive cutter locations. This approximation is similar to the actual tool motion generated by a CNC controller. The next step is to intersect the lines with the peripheral surface of the cutter. The geometrical deviations are calculated as the sum of the lengths of the trimmed straight lines. The sampling density in the stock height method controls the estimation precision of the accumulated geometrical deviations. This factor is also used to determine the computational time required in the optimization process.

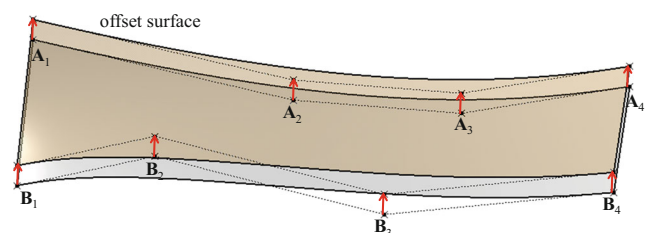
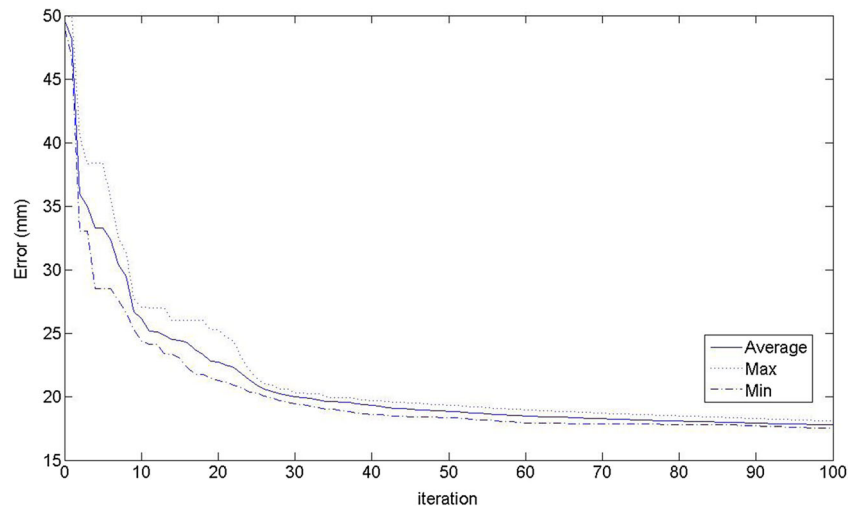


**Fig. 4** Initial solution is determined from the offset surface

**Fig. 5** The convergence curves of the current optimization scheme



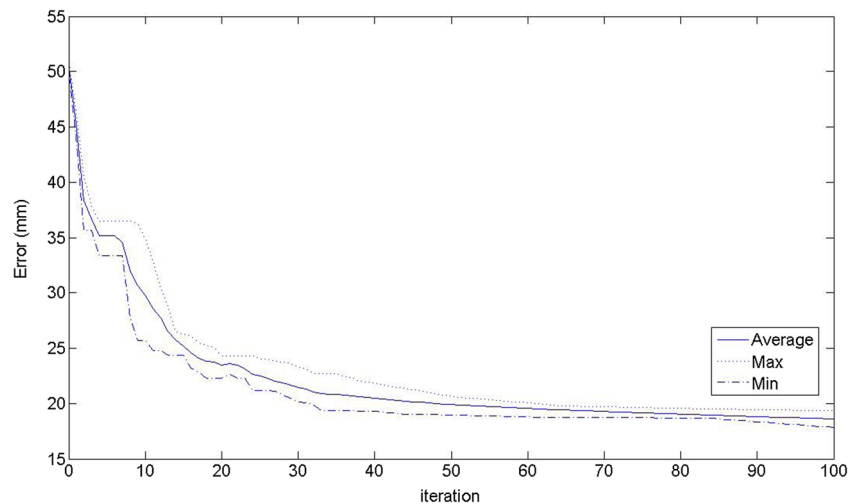
Estimating the objective function does not entail a closed-form representation or analytical solutions. Derivative-based non-linear optimization techniques are thus not applicable to searching for optimal solutions. Metaheuristic algorithms, such as PSO, normally work more effectively in this situation. Detailed descriptions of the PSO algorithm can be referred to previous studies [2, 8] and thus are omitted in this paper.

The objective function (or fitness function) in the PSO algorithms is written as follows:

$$\text{Min} \sum_{i=0}^{N-1} \epsilon \left( \mathbf{CL}_i \xrightarrow{M} \mathbf{CL}_{i+1} \right) \quad (2)$$

where  $\epsilon$  is the geometrical deviation induced by the cutter motion  $M$  from  $\mathbf{CL}_i$  to  $\mathbf{CL}_{i+1}$ . A tool path consists of  $N$  cutter locations. The geometrical deviations are calculated as the sum of the lengths of the trimmed straight lines [6]. The sampling density in the method controls the estimation precision of the deviations and the computational time required in the optimization process. The objective function is thus approximated as follows:

**Fig. 6** The convergence curves of the previous optimization scheme



$$\text{Min} \sum_i \epsilon^* \left( \mathbf{CL}_i \xrightarrow{\text{interpolation}} \mathbf{CL}_{i+1} \right) \quad (3)$$

where  $\epsilon^*$  is the approximate deviations estimated by the stock height method. A set of intermediate cutter locations linearly interpolated from  $\mathbf{CL}_i$  to  $\mathbf{CL}_{i+1}$  replaces the continuous tool motion. Thus, the objective function estimates the accumulated machining deviations on the finished surface by the stock height method using CNC linear interpolation.

Table 1 lists the machining parameters in the proposed tool-path planning method, and Table 2 lists the parameter setting in the PSO algorithm. For comparison, a tool path contains 40 cutter locations, as in a previous research [11]. The parameter setting used in the PSO algorithm also remains identical. The inertia weight and two learning factors were determined through trial and error. The number of interpolations specifies how many intermediate tool positions are used in estimating the machining deviations between cutter locations.

A test ruled surface is defined according to two boundary curves; their control points are shown in Fig. 3. Each boundary is specified as a cubic Bézier curve in 3D space. PSO

**Table 3** Test results generated using different methods

	Overcut (mm)	Undercut (mm)	Total deviations (mm)
Spline-constrained tool path	9.310	8.401	17.711
Non-constrained tool path	11.094	7.528	18.622

requires an effective initial solution to attain favorable search results. Offsetting the boundary curves along a given direction at their control points at a distance of the tool radius (Fig. 4) yields a new ruled surface. Varying the curve parameter value by an equal interval produces a set of surface rulings. Each ruling corresponds to a cutter location when the end points along the normal directions are offset. Thus, the generated tool path is applicable as a favorable initial solution in the PSO algorithm.

### 3 Test results

Both simulation and real machining tests were conducted to verify the proposed method. The PSO algorithm was conducted five times at the given parameter settings (Tables 1 and 2) to reduce the randomness involved in the search process. Figure 5 shows the convergence curves for the best, worst, and average results in 100 iterations. All five runs converged to optimal solutions, although their processes appear slightly different. The PSO algorithm that adjusts the tool path without the motion constraint was also tested under the same

conditions. The corresponding convergence curves are presented in Fig. 6. Table 3 lists the final solutions generated using both methods. The optimal tool path constrained by spline curves produces a lower number of geometrical deviations than that consisting of independent cutter locations does. Figure 7a, b indicates the non-constrained and constrained tool paths, respectively. The line segment at each cutter location represents the tool axis that connects the two end points of the cutter. The spline tool path must be converted into G01 motions because current CNC controllers do not support spline interpolation in five-axis flank machining defined according to two curves. As in the non-constrained tool path, 40 cutter locations are generated from the spline path for actual machining. The parameter value in both curve equations is varied from 0 to 1 with an increment of 0.025. Each parameter value thus produces two tool center points. Connecting the two points determines a cutter location in G01.

The term “minimized” indicates that the objective function in the optimization method employed to generate tool paths in this paper is to minimize the geometrical deviation on the machined surface. The PSO approach used to determine the non-constrained tool path actually outperforms all the other methods referred in Section 1 (see Refs [2] and [8]). We thus compared the spline-constrained tool path only with this best method.

A cutting experiment was conducted to verify the simulation results. A Deckel-Maho nanoBlock™ five-axis CNC machine tool was used in this experiment. The moving range of the worktable is 780×560×560 mm. The maximal spindle speed is 12,000 RPM. The machining operation consists of roughing and finishing cuts. The roughing cut involved using a  $\phi 4$  ball-ended cylindrical cutter with a total length of 30 mm and a cutting length of 20 mm. This operation enabled removing most stock materials and left a material layer 0.2 mm thick on the design surface, to be removed by the finishing cut. A new tool of the same type as that used in the roughing cut was adopted in the finishing cut to eliminate the influence of tool wear. The cutting conditions in the finishing cut, suggested by the cutter provider, are summarized in Table 4. The cutting length can cover the entire surface along the shorter side (see Fig. 3); thus, the finishing cut requires only one tool path.

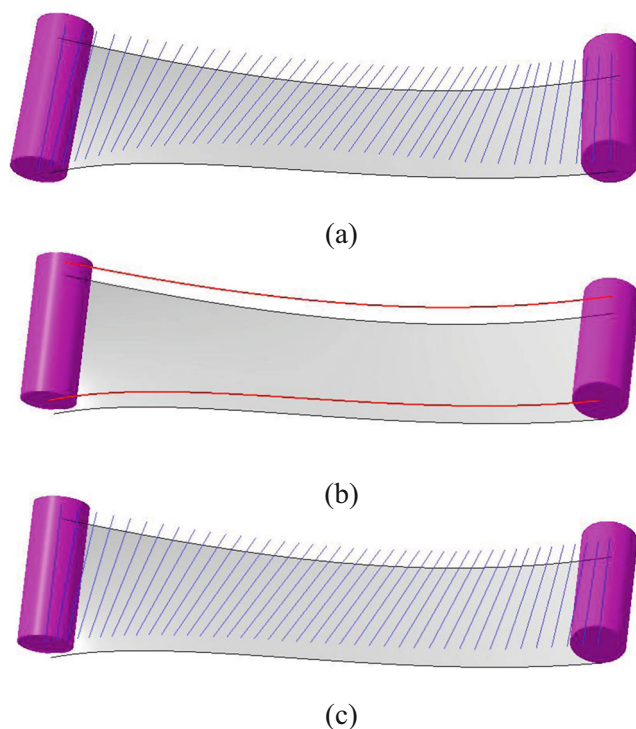
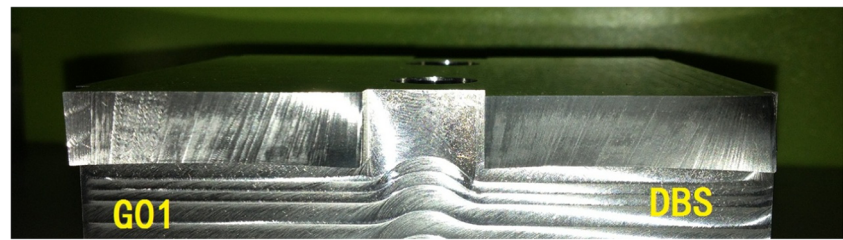


**Fig. 7** Optimized tool paths **a** non-constrained tool path, **b** spline-constrained tool path, and **c** linearized motion of **b**

**Table 4** Cutting conditions in the finishing cut

Work material	Al 6060-T5
Spindle speed	10,000 RPM
Feedrate	500 mm/min
Depth of cut	0.2 mm

**Fig. 8** The left and right surfaces were machined using non-constrained and spline-constrained tool paths, respectively (*DBS* indicates the tool path defined by two splines)



As shown in Fig. 8, the finished part consists of two surfaces; each of which was cut by either the non-constrained or spline-constrained tool path with the same condition shown in Table 4. *DBS* (*Double Spline*) in the figure indicates the tool path defined by two splines. An emulsion of water with mineral oil was used as a cutting fluid in both cuts. The geometrical deviations of both surfaces according to the design specifications were measured using the Form Talysurf<sup>TM</sup> PGI 1250A surface scanner with a 0.8-nm resolution. The stylus of this device moves along predefined trajectories on the surface to be measured. With respect to a reference point, the 3D coordinates can be automatically determined at discrete measurement positions along each trajectory. Nine isoparametric curves were created based on the design surface along the  $v$ -direction of the scanning trajectories. Each curve contains 280 measurement points of equal increments within the curve parameter along the  $u$  direction (Fig. 9). No measurement points were generated near the surface boundaries, to avoid possible stylus collision around these regions. The measurement results for both surfaces are listed in Table 5. The stylus reports the 3D position at each measurement point. The deviation at each point is then estimated by projecting the reported position back to the design specifications in CAD. A calibration procedure was applied to align the origin for both the finished part and the design geometry.

The results revealed that the spline-constrained tool produces smaller machining deviations than those of the unconstrained tool path. The new path planning method produces a higher machining quality when the geometrical deviation is considered. However, the measured values differed from the simulation results (Table 3). As explained in previous studies [5, 6], a major reason for the difference is that the number and distribution of the sampling points in the simulation differ

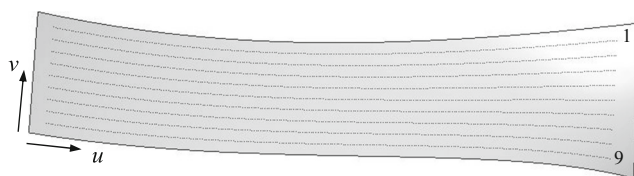


**Fig. 9** Distribution of measurement points on the machined surface

from those in the actual measurement. Tool deflection during the machining is another possible reason [12]. However, it should not be the dominating factor in the finishing cut as in this case, which involves light cutting loads.

Quantitative evidence can be further derived from the measurement as the arithmetic average of surface roughness  $R_a$ :

$$R_a = \frac{1}{n} \sum_{i=1}^n |y_i| \quad (4)$$

where  $n$  is the number of sampling points along a base length  $L$  and  $|y_i|$  is the deviation at the  $i$ th sampling point with respect to the ideal profile on the surface. The deviation can be directly read from the surface scanner. The surface roughness is estimated using (4) for each scanning trajectory in the measurement. As indicated by Table 6, the surface roughness produced by the spline-constrained tool path is superior to that of the non-constrained tool path in all scanning trajectories (see Fig. 9 for the number of scanning trajectory). Also note that the surface roughness increases from scanning trajectory 1 to 9. The tool was clamped on the side of trajectory 1. Near the side of trajectory 9 was a free end, subject to a greater amount of possible tool chatter than the other side.

A schematic drawing was generated for visualizing and comparing the surface quality of both machined surfaces. The  $z$ -coordinate value of each scanning point was increased tenfold. The  $x$ - and  $y$ -coordinates were then replaced by the  $u$  and  $v$  values in the parameter space. Although lacking correct proportions in dimensions, the scanning profiles thus exhibited fewer height variations on the surface machined by the constrained tool path (Fig. 10). The surface quality is substantially improved compared with that produced by the unconstrained tool path, mainly because of the continuity of the optimal tool path imposed by spline curves. This constraint

**Table 5** The geometrical deviations measured by a surface scanner

	Total deviations (mm)
Spline-constrained tool path	44.895
Non-constrained tool path	47.566

**Table 6** Surface roughness estimated from the surface scanner

Scanning trajectory	Surface roughness $R_a$ ( $\mu\text{m}$ )	
	Constrained tool path	Unconstrained tool path
1	3.760	8.751
2	4.435	9.123
3	6.079	9.790
4	7.134	11.125
5	6.880	12.910
6	8.293	13.083
7	11.664	12.921
8	10.543	15.466
9	13.098	13.402

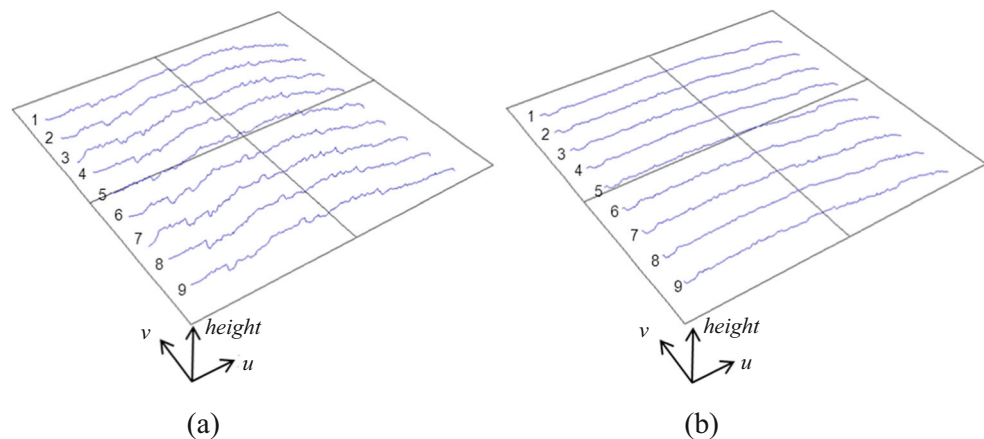
effectively prevents the tool orientation from causing excessive changes during the optimization process.

To discuss the degree of the spline curve used in the constrained tool path is important. Our previous study (Ref [13]) proposed a similar approach to improving surface developability by spline-based re-parameterization techniques. The test results show that increasing the degree of the spline curve improves the optimal solutions while requiring a longer computational time. Another finding was that increasing the developability of the envelope surface sweeping along a tool path has a direct impact on reducing the geometrical deviation on the machined surface. We chose cubic splines because their computational complexity is lower than that of degree 5 or 7. Moreover, the test ruled surface was constructed with two cubic Bezier curves. Tool paths constrained by quadratic curves may fail to produce satisfactory results due to insufficient non-linearity in the tool motion.

## 4 Conclusion

Previous studies have shown that geometrical deviations of a surface produced using five-axis flank machining can be reduced by optimizing the finishing tool path. Several optimization schemes have been developed to simultaneously adjust cutter locations driven by minimizing the deviations. However, the optimized tool path can sometimes yield low surface quality on the finished part induced by abrupt changes of the tool axis. For overcoming this problem, this paper proposes a new optimization scheme for tool-path planning that minimizes the degree of geometrical deviations while improving the surface roughness of the machined result. The tool path is constrained by spline curves in the proposed scheme. The optimization process entails searching for the optimal coefficients of the polynomial equations describing the curves. A five-axis machining experiment was conducted to produce surfaces by using two tool paths, one with and one without the spline motion constraint. The results measured using a surface scanner revealed that the constrained tool path produces superior surface roughness to that of the non-constrained tool path. The continuity imposed by the spline motion reduces uneven modifications of cutter locations during the optimization process. This paper provides an effective approach for minimizing the degree of geometrical deviations in the five-axis finishing of a ruled surface while maintaining high surface quality on the machined part. Future research will entail integrating cutting models in tool-path planning to resolve other machining challenges such as avoiding chatter and reducing energy consumption. To understand how the degree of the spline influences the surface quality is also worth of further studies.

**Fig. 10** A schematic drawing helps visualize the surface quality of two machined surfaces **a** non-constrained tool path and **b** constrained tool path



## References

1. Harik RF, Gong H, Bernard A (2013) 5-axis flank milling: a state-of-the-art review. *Comput Aided Des* 45(3):796–808
2. Hsieh HT, Chu CH (2012) Optimization of tool path planning in 5-axis flank milling of ruled surfaces with improved PSO. *Int J Precis Eng Manuf* 13(1):77–84
3. Landon Y, Segonds S, Lascoumes P, Lagarrigue P (2004) Tool positioning error (TPE) characterization in milling. *Int J Mach Tools Manuf* 44:457–464
4. Tsay DM, Her MJ (2001) Accurate 5-axis machining of twisted ruled surfaces. *ASME J Manuf Sci Eng* 123:731–738
5. Chu CH, Lee CT, Tien KW, Ting CJ (2011) Efficient tool path planning for 5-axis flank milling of ruled surfaces using ant colony system algorithms. *Int J Prod Res* 49(6):1557–1574
6. Wu PH, Li YW, Chu CH (2008) Optimized tool path generation based on dynamic programming for five-axis flank milling of rule surface. *Int J Mach Tools Manuf* 48(11):1224–1233
7. Wu, Q, Li, X, Gao, L, Li, Y (2013) A simplified electromagnetism-like mechanism algorithm for tool path planning in 5-axis flank milling. *IEEE 17th International Conference on Computer Supported Cooperative Work in Design*, pp 422–426
8. Chu CH, Hsieh HT (2012) Generation of reciprocating tool motion in 5-axis flank milling based on particle swarm optimization. *J Intell Manuf* 23(5):1501–1509
9. Chu CH, Wu PH, Lei WT (2012) Tool path planning for 5-axis flank milling of ruled surfaces considering CNC linear interpolation. *J Intell Manuf* 23(3):471–480
10. Chu CH, Chen JT (2006) Tool path planning for five-axis flank milling with developable surface approximation. *Int J Adv Manuf Technol* 29(7–8):707–713
11. Hsieh HT, Tsai YC, Chu CH (2013) Multi-pass progressive tool path planning in five-axis flank milling by particle swarm optimization. *Int J Comput Integr Manuf* 26(10):977–987
12. Chen KH (2011) Investigation of tool orientation for milling blade of impeller in five-axis machining. *Int J Adv Manuf Technol* 52(1–4):235–244
13. Chu CH, Cheng KC (2013) Precise 5-Axis grooving of tire mold by optimization of surface developability. *Int J Precis Eng Manuf* 14(10):1–6